Immunity, Vol. 17, 639–651, November, 2002, Copyright ©2002 by Cell Press

The "Dispensable" Portion of RAG2 Is Necessary for Efficient V-to-DJ Rearrangement during B and T Cell Development

Hong-Erh Liang,[1,2] Lih-Yun Hsu,[1,2] Dragana Cado,[1] Lindsay G. Cowell,[3] Garnett Kelsoe,[3] and Mark S. Schlissel[1,4]
[1]Department of Molecular & Cell Biology
Division of Immunology
University of California
Berkeley, California 94720
[2]Graduate Program in Immunology
Johns Hopkins University School of Medicine
Baltimore, Maryland 21205
[3]Duke University Medical Center
Department of Immunology
Durham, North Carolina 27710

Summary

Previous in vitro studies defined the minimal regions of RAG1 and RAG2 essential for V(D)J recombination. In order to characterize the role of the C-terminal "dispensable" portion of RAG2, we generated core-RAG2 knock-in mice. We found that the core-RAG2-containing recombinase complex is selectively defective in catalyzing V-to-DJ rearrangement at the IgH and TCRβ loci, resulting in partial developmental blocks in B and T lymphopoiesis. Analysis of recombination intermediates showed defects at the cleavage phase of the reaction. We also observed a reduction in overall recombinase activity in core-RAG2-expressing thymocytes, leading us to suggest that the interaction of a defective recombinase with RSS sequences unique to VH and Vβ gene segments may underlie the specific V-to-DJ rearrangement defect in core-RAG2 mice.

Introduction

Immunoglobulin (Ig) and T cell receptor (TCR) gene variable exons are assembled by a series of site-specific recombination reactions called V(D)J recombination (Fugmann et al., 2000; Hesslein and Schatz, 2001). Rearranging gene segments are flanked by recombination signal sequences (RSSs) consisting of a conserved heptamer and nonamer separated by spacer DNA of conserved length (either 12 or 23 nucleotides) but not sequence. RSSs are recognized by a common recombinase machinery containing two lymphoid-specific factors, RAG1 and RAG2. Both RAG1 and RAG2 have been subjected to extensive mutational analyses which led to the identification of the catalytic center of the RAG complex, a DDE motif, located within RAG1. This active site motif resembles the catalytic domain of bacterial transposases and retroviral integrases. In addition, RAG1 contains the sequence-specific DNA binding domain involved in RSS recognition and also contributes most of the DNA contacts to the RSS-heptamer and the adjacent coding segment (Akamatsu and Oettinger, 1998; Eastman et al., 1999; Swanson and Desiderio, 1998, 1999). Hence, RAG1 plays a central role in RSS recognition, catalysis, and assembly of the basal recombinase complex.

In contrast, despite being absolutely indispensable for activity of the recombinase, the precise role of RAG2 in V(D)J recombination has remained elusive. The only known specific role for RAG2 is to increase the stability and specificity of interactions between RAG1 and the RSS (Akamatsu and Oettinger, 1998; Swanson and Desiderio, 1998), but not through direct, sequence-specific interaction with DNA (Eastman et al., 1999; Mo et al., 1999; Swanson and Desiderio, 1998). Although all conserved acidic residues within RAG2 are dispensable for catalytic activity of the RAG complex (Landree et al., 1999), several basic residues of RAG2 have been shown to be critical for the ability of the recombinase to form and open coding-end hairpins in vitro (Qiu et al., 2001), as well as for DNA substrate recognition by RAG1/2 complex (Fugmann and Schatz, 2001).

Since full-length RAG1 and RAG2 are insoluble at physiological salt concentrations, all biochemical studies of RAG1 and RAG2 have relied on truncated, catalytically active recombinant proteins, which are readily soluble. These core-RAG1 (amino acids 384–1008 of 1040 residues) and core-RAG2 (amino acids 1–383 of 527 residues) proteins were initially defined as the minimal regions of each protein essential for near-wild-type recombination activity on cotransfected extrachromosomal reporter substrates in nonlymphoid cell lines (reviewed in Fugmann et al., 2000). Despite their apparent dispensability, the non-core regions of RAG1 and especially RAG2 are evolutionarily conserved, suggesting that they may play important roles in the assembly of endogenous Ig and TCR genes during lymphoid development. These roles may include quantitative or qualitative regulation of RAG activity (Kirch et al., 1998, 1996; McMahan et al., 1997; Roman et al., 1997; Steen et al., 1999), perhaps specifically suppressing aberrant recombination (Sekiguchi et al., 2001). In addition, RAG2 is subject to cell-cycle-dependent degradation, and the conserved amino acids responsible for this posttranslational regulatory mechanism lie within the non-core region of RAG2 (Li et al., 1996).

In an attempt to identify the function of the non-core region of RAG2, Kirch et al. (1998) studied the regulation of V(D)J recombination by transfection of either full-length or core-RAG2 into RAG2 null Abelson virus-transformed pro-B cell lines. While core-RAG2 was less active than full-length RAG2 in this assay system, these workers reported a disproportionate effect of the deletion on heavy-chain V-to-DJ_H as compared to D-to-J_H or V-to-J_K rearrangement. Previous work had shown, however, that V(D)J recombination is not appropriately regulated in v-*abl* transformed cell lines (Schlissel et al., 1991), thus limiting the significance of these results.

In this study, we explore the importance of the non-core region of RAG2 in regulating V(D)J recombination at endogenous Ig and TCR loci by generating and analyzing core-RAG2 knock-in mice.

[4]Correspondence: mss@uclink4.berkeley.edu

Results

Generation of Core-RAG2 Knock-In Mice

To generate mice expressing only core-RAG2 protein, we used homologous recombination to replace the full-length RAG2 coding sequence with core-RAG2 (Figure S1A [http://www.immunity.com/cgi/content/full/17/5/639/DC1]). To preserve as closely as possible the endogenous regulation of *RAG2* at the posttranscriptional level, the 3′ untranslated region (UTR) of *RAG2* was retained 3′ of the truncated gene to provide polyadenylation signals and to maintain normal RNA metabolism.

We used the Cre-*loxP* strategy (Naramura et al., 1998) to achieve deletion of the floxed-*neo*^{r} gene in vivo by crossing chimeras generated from core-*RAG2-NEO* targeted ES clones (+/N) with Cre recombinase transgenic mice (Figure S1B [http://www.immunity.com/cgi/content/full/17/5/639/DC1]), resulting in mice carrying only the core-RAG2 mutation and a *loxP* site between the core-RAG2 stop codon (aa 384) and the endogenous 3′ UTR (Figure S1A). Subsequent mating of heterozygous (+/Δ) mice generated wild-type *RAG2* (+/+), heterozygous core-*RAG2* (+/Δ), and homozygous core-*RAG2* (Δ/Δ) mice for analysis (Figure 1A). Hemizygotes with full-length (+/−) or core-*RAG2* (Δ/−) were also generated by crossing *RAG2* null (−/−) with heterozygous core-*RAG2* (+/Δ) mice (Figure S1C). To assess the expression of core-RAG2 protein in the mutant mice, we performed Western blot analysis on adult thymocyte whole-cell lysates (Figure 1A). A polyclonal antiserum (Lin and Desiderio, 1993) against a murine RAG2 N-terminal peptide (aa 156–171) was used since this epitope exists in both full-length and core-RAG2. Although transcription of the core-*RAG2* gene is regulated by endogenous sequences, we observed an increase in steady-state amounts of core-RAG2 protein compared to wild-type RAG2 protein. Taking into consideration the increase in DN cells and slight reduction in DP cells observed in mutant thymocytes (see below), we concluded that, on a single-cell basis, there is at least 2-fold more core-RAG2 protein in mutant thymocytes than full-length RAG2 in wild-type thymocytes. Removal of the C terminus of RAG2 eliminates its well-characterized degradation signal (Li et al., 1996), and thus the prolonged half-life of core-RAG2 likely contributes to its accumulation in developing thymocytes.

We observed a reduction of cellularity in bone marrow, spleen, and thymus in animals carrying the core-*RAG2* mutation (Figure S1C [http://www.immunity.com/cgi/content/full/17/5/639/DC1]). Except for a reduction of mature splenic B cells in hemizygous core-RAG2 mice, there was no significant difference in the ratio of T and B cell populations, the percentage of $CD4^+$ and $CD8^+$ populations, or the percentages of $CD4^+CD8^+$ and pre-B ($B220^+IgM^-$) cells in the spleen (data not shown), suggesting that the truncation of RAG2 most likely affects early lymphocyte development.

A Partial Block in B Lymphocyte Development and *Ig* Gene Rearrangement in Core-RAG2 Mice

B lymphopoiesis is impaired at an early stage in the bone marrow of core-RAG2 mice (Figure 1). While the number of $CD43^+B220^+IgM^-$ pro-B cells is normal (Figure 1B), there is an ~4-fold reduction in the number of pre-B cells ($CD43^-B220^+IgM^-$) and in surface IgM^+ B lymphocytes compared to wild-type littermates (Figure 1B). The attenuation of development at the pro-B to pre-B transition and reduction in IgM^+ B cells is also reflected by flow cytometric analysis (Figure 1C). This partial developmental block occurs at the stage when developing B cells are assembling their Ig heavy-chain (IgH) gene. Productive complete heavy-chain gene rearrangement is required for progression from the pro-B to the pre-B stage of development (Hesslein and Schatz, 2001). As shown in Figure S1D (http://www.immunity.com/cgi/content/full/17/5/639/DC1), the numbers of total nucleated bone marrow cells and thymocytes in the core-RAG2/null hemizygote (Δ/−) are more affected than core-RAG2 homozygote (Δ/Δ). This dosage effect of core-RAG2 protein suggests that the deleterious effect caused by truncation of the *RAG2* gene might be related to reduced recombinase activity. It is also notable that the core-RAG2 heterozygote (+/Δ) mice show a modest block at the pro-B to pre-B transition as evidenced by an increased percentage of $CD43^+$ $B220^+$ cells while the RAG2 null heterozygote (+/−) exhibits no such block (Figure 1C and data not shown). This observation suggests that core-RAG2 protein can interfere with the function of wild-type RAG2.

To determine if IgH gene assembly is affected in core-RAG2 mice, we sorted pro-B cells from core-RAG2 animals and wild-type controls. The extent of DJ_H joining in pro-B cells was measured by a standard semiquantitative PCR strategy (Schlissel et al., 1991). We found that D-to-J_H recombination proceeds in an indistinguishable fashion in pro-B cells expressing either full-length or core-RAG2 proteins (Figure 2A). In contrast, V_H-to-DJ_H joining is severely impaired in core-RAG2 pro-B cells (Figure 2B). Unlike the progressive impairment of V_H-to-DJ_H rearrangement observed in IL-7Rα-deficient mice (Corcoran et al., 1998), core-RAG2 mice are defective in mediating V-to-DJ rearrangement across the entire IgH locus regardless of the distance between the specific V_H family and downstream DJ_H segment (Figure 2B). This global defect results in a ~10-fold reduction in the frequency of complete heavy-chain gene assembly (Figure 2C).

To determine whether a similar defect exists with other rearranging loci, pre-B cell DNA was assayed by PCR for $VJ\kappa$ rearrangements. Analogous to D-to-J_H rearrangement, we found no effect of the absence of the RAG2 C terminus on rearrangement at the Igκ locus (Figure 2D). Since $V\kappa$-to-$J\kappa$ rearrangement occasionally precedes the completion of IgH gene assembly, we also compared V-to-$J\kappa$ joining events mediated by full-length and core-RAG2 in pro-B cells. We detected comparable levels of $VJ\kappa$ rearrangement in wild-type and mutant pro-B cells, suggesting that the defect in IgH V-to-DJ rearrangement is specific to that particular rearrangement event and not the pro-B cell stage of development itself (data not shown).

Reduced V_H-to-DJ_H Recombination Reaction Intermediates in Pro-B Cells from Core-RAG2 Mice

Recombination intermediates (broken signal ends, SBE) within the IgH and IgL loci were examined using a pre-

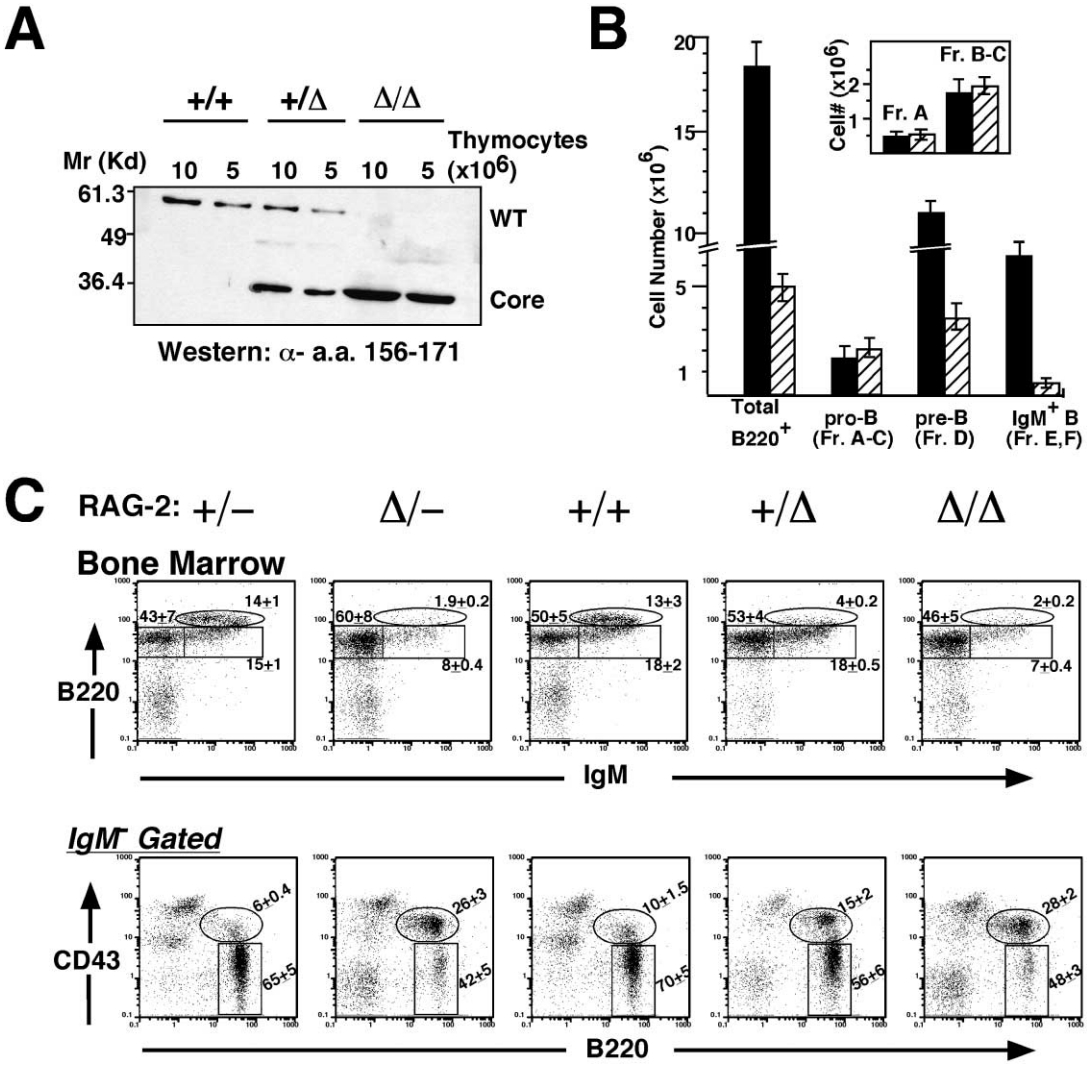

Figure 1. B Cell Development in Core-RAG2 Knock-In Mice

(A) Full-length RAG2 and core-RAG2 protein expression in the thymus. An anti-N′RAG2 Western blot analysis of adult thymocyte lysates from the indicated genotypes is shown with the positions of wild-type (WT) and core-RAG2 mutant (core) proteins indicated.

(B) Size of developing B cell subpopulations from wild-type (+/+, solid bars) and core-RAG2 (Δ/Δ, hatched bars) mice. RBC-free bone marrow cells from both femurs and tibiae of individual mouse were analyzed by flow cytometry, and developmental fractions were determined according to Hardy's scheme (Hardy et al., 1991). Data represent the means and standard deviation (error bars) from six independent analyses. Insert, cell numbers of early pro-B fractions (Fr. A and B/C) in wild-type and core-RAG2 BM were further determined by HSA staining (N = 2).

(C) FACS analysis of BM cells from hemizygous (+/−, Δ/−) mice and wt (+/+), heterozygous (+/Δ), or homozygous core-RAG2 (Δ/Δ) littermates stained with FITC-anti-IgM, PE-anti-B220, and bi-anti-CD43 followed by SA-QR. Pro-B and pre-B cells were further distinguished by CD43 marker expression (lower panel) as in Hardy et al. (1991). IgM^- gated cells are shown as fraction A-C pro-B cells ($B220^+CD43^+$) and fraction D pre-B cells ($B220^+CD43^-$). Percentages in each case represent the means and standard deviations of live-gated subpopulations from six mice of each genotype.

viously described LMPCR approach (Schlissel et al., 1993). Figure 2E shows that dsDNA breaks 5′ of D_H RSS, which are associated with V_H-to-DJ_H rearrangement, were dramatically reduced in DNA purified from core-RAG2-expressing pro-B cells, whereas dsDNA breaks derived from the 3′ of D_H RSS, which are associated with D_H-to-J_H assembly, were not affected. Intermediates derived from κ or λ light chain rearrangements involving 5′Jκ1 23-RSS and 5′Jλ 12-RSS were also unaffected. This indicates that the core-RAG2-containing V(D)J recombinase fails to efficiently initiate RSS cleavage 5′ of D_H RSS in the IgH locus, resulting in the impairment of V_H-to-DJ_H rearrangement in mutant pro-B cells.

Despite its defect in initiating V_H-to-DJ_H rearrangement, core-RAG2 apparently preserves the ability to respond to stage-specific developmental regulatory cues. We observed neither precocious Jκ or Jλ RSS cleavage in core-RAG2 pro-B cells nor the extension of D_H RSS cleavage into the pre-B cell stage (Figure 2E). Quantification of 5′D_H SBEs revealed that core-RAG2 has an

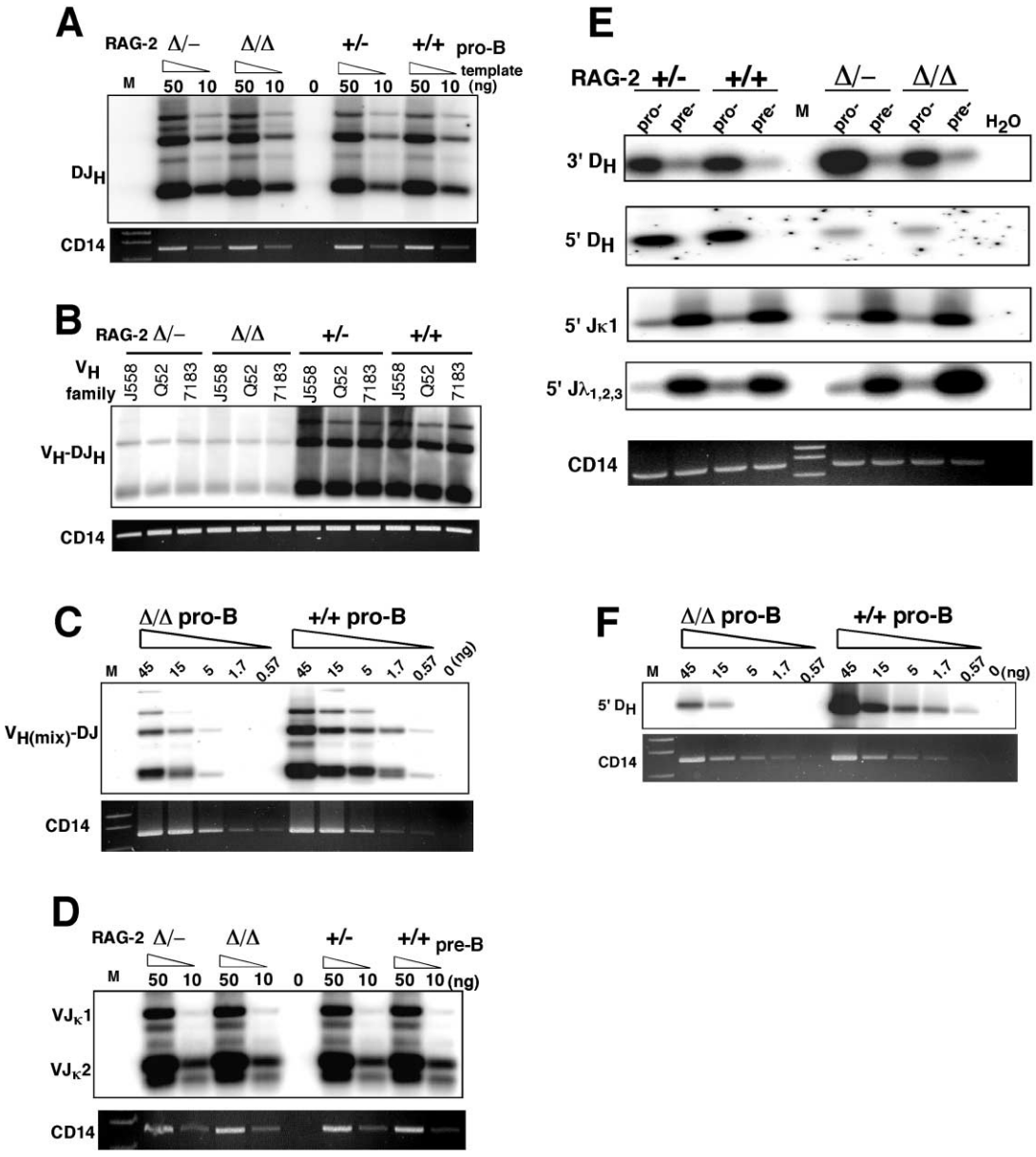

Figure 2. Impaired V_H-to-DJ_H Rearrangement in Pro-B Cells Expressing Core-RAG2

(A) PCR analysis of D_H-to-J_H rearrangement was performed on the indicated amounts of genomic DNA purified from FACS-sorted pro-B cells from homo- or hemizygous wild-type or core-RAG2 knock-in mice. A Southern blot of PCR products is shown, probed with an oligo specific for the J_H region. The lower panel shows control amplifications of a nonrearranging genomic locus (CD14; EtBr stained gel photograph).

(B) Pro-B cell genomic DNA from mice of the indicated genotypes was amplified by PCR using three sets of degenerate primers corresponding to V_HJ558 (D_H-distal), V_HQ52, and V_H7183 (D_H-proximal) segments in combination with a single J_H primer to detect V_H-to-DJ_H rearrangements spanning the IgH locus. The Southern blot shown was probed as in (A).

(C) Three-fold serially diluted genomic DNA samples from homozygous core-RAG2 (Δ/Δ) or wt (+/+) pro-B cells were amplified with an equal-molar mixture of degenerate V_HJ558, V_HQ52, and V_H7183 primer set (V_{Hmix}) paired with a single J_H primer. A Southern blot is shown as in (B).

(D) Either 50 ng or 10 ng of genomic DNA from sorted pre-B cells was amplified with a degenerate V_k primer and a primer downstream of the J_k2 segment. A probe derived from Jκ2 coding sequence was used to detect amplified VJ_k rearrangements by Southern blot.

(E) LMPCR was used to detect RSS signal ends generated by the full-length or core-RAG2 recombinase complex at either the pro-B or pre-B stage of B cell development. Shown are the analyses of the 3′ D_H and 5′ D_H 12-RSS, the 5′ Jκ1 23-RSS, and the 5′ $J_λ$ 12-RSS broken signal end (SBE) amplified products. CD14 denotes direct PCR amplification of a control locus using linker-ligated DNA.

(F) LMPCR of 3-fold serially diluted linker-ligated DNA from mutant (Δ/Δ) or wt (+/+) pro-B cells was used to compare the amounts of 5′ D_H signal ends generated by full-length or core-RAG2.

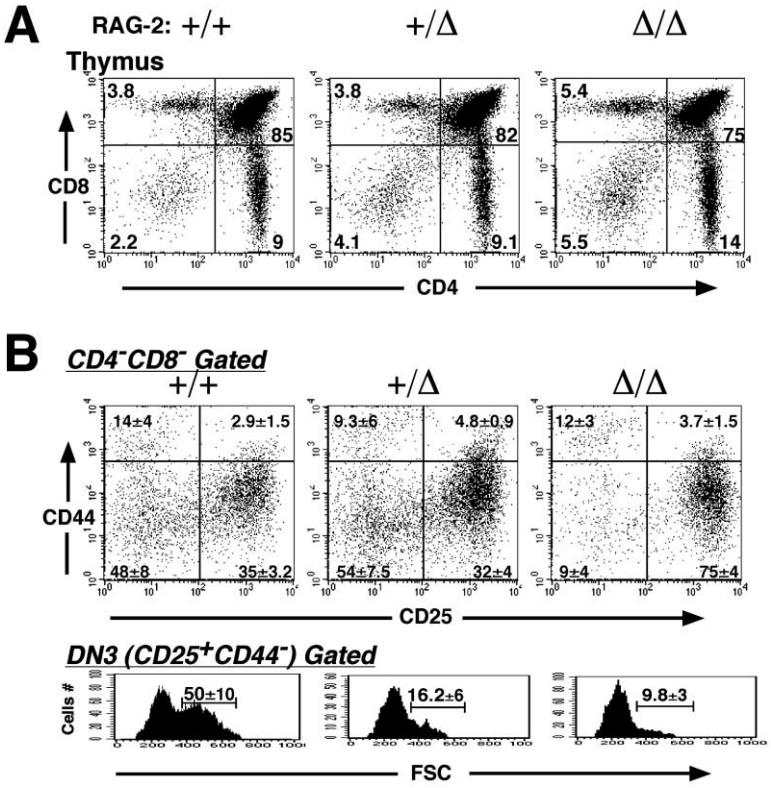

Figure 3. T Cell Development in Core-RAG2 Knock-In Mice

(A) Thymocytes from mice of the indicated genotypes were stained with FITC-anti-CD4 and PE-anti-CD8.

(B) Thymocytes were stained with FITC-anti-CD4, FITC-anti-CD8, PE-anti-CD25, and Cyc-anti-CD44. Upper, distribution of gated $CD4^-/CD8^-$ thymocytes from various genotypes. Percentages indicated in each quadrant are the mean and standard deviation of five independent repetitions of this experiment. Lower, histogram displaying forward scatter analysis of DN3 ($CD25^+CD44^-$) cells of each genotype. The gate indicates the percentage of "large" (cycling) cells.

~20-fold reduction in RSS cleavage efficiency relative to full-length RAG2 (Figure 2F) which correlates with the observed reductions in V_H-to-DJ_H rearrangements and the production of pre-B cells.

T Cell Development in Core-RAG2 Mice

The physiologic consequences of the absence of the RAG2 C terminus on developing T cells were examined in thymocytes from core-RAG2 mice and their littermates. We found that the CD4 and CD8 staining profiles were similar for core-RAG2 (Δ/Δ) mice and wild-type littermate (+/+) controls (Figure 3A), except for an attenuation of the DN to DP transition, resulting in a modest accumulation of DN cells in core-RAG2 mice.

In order to assess the significance of this increased fraction of DN cells, we proceeded to analyze DN thymocytes using antibodies to CD25 and CD44. We found a partial but significant block in core-RAG2 thymocyte development at the transition from the $CD25^+CD44^-$ DN3 stage to the $CD25^-CD44^-$ DN4 stage (Figure 3B). We also observed a striking reduction in the percentage of large cycling cells within the DN3 population of core-RAG2 thymocytes (Figure 3B, bottom; also revealed by measurements of the percentage of cells in the S and G2/M phases of the cell cycle after DNA content staining, data not shown). At the DN3 stage, productive V-to-DJβ gene rearrangement leads to expression of the pre-TCR on the cell surface and consequent pre-TCR signaling permits cell survival, proliferation, and differentiation (reviewed in von Boehmer et al., 1999). As a result, the DN3 population is selected for in-frame TCRβ rearrangement, a process called β-selection. The developmental phenotype observed in core-RAG2 mice suggests that, despite the accumulation of core-RAG2 protein in thymocytes (Figure 1A), mutant DN3 cells have difficulty assembling a complete TCRβ chain.

Impaired Vβ-to-DJβ Rearrangement Mediated by Core-RAG2

To elucidate the underlying mechanism causing this partial developmental block at the DN3 to DN4 transition, we compared the frequency of TCRβ rearrangements in sorted DN3 T cells from wild-type and core-RAG2 mice. Similar to the defect observed in IgH rearrangement, core-RAG2 is defective in Vβ-to-DJβ rearrangement but mediates normal Dβ-to-Jβ joining (Figures 4A and 4B). Using different Vβ gene-specific primers, including ones specific for the most distal Vβ2 gene (~650 kb upstream of the Dβ elements) and the proximal Vβ14 gene (~10 kb downstream of the Cβ2 region), we found that Vβ-to-DJβ rearrangement involving Vβ segments across the entire locus was impaired in mutant DN3 cells (~4-fold reduction, Figure 4B). We used LMPCR to determine whether diminished Vβ-to-DJβ rearrangement is due to a defect at the cleavage or at a postcleavage step of the reaction. Figures 4D and 4E show that cleavage of the 3′Dβ 23-RSS was not affected by the core-RAG2 mutation as measured by the abundance of SBE. In contrast, core-RAG2-mediated cleavage of 5′Dβ 12-RSS was reduced corresponding to the defect observed in Vβ-to-DJβ rearrangement (Figures 4C and 4D). We went on to compare the levels of SBE at two specific Vβ 23-RSS sequences in wild-type and core-RAG2 mutant DN3 and DN4 thymocytes. In

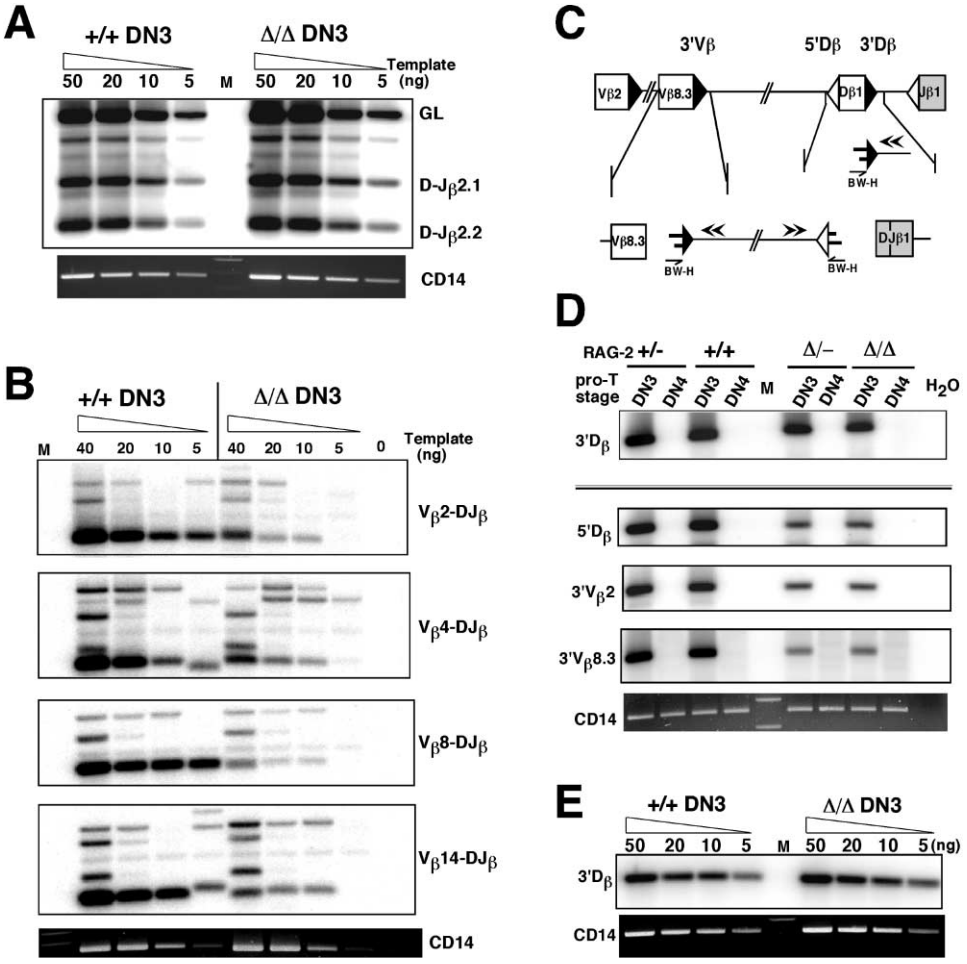

Figure 4. Impaired Vβ-to-DJβ Rearrangement in Pro-T Cells Expressing Core-RAG2

(A) Indicated amounts of DNA purified from sorted DN3 cells from wild-type or core-RAG2 littermates were analyzed by PCR for Dβ2-to-Jβ2.1 or -Jβ2.2 rearrangement. GL indicates the PCR product from the germline TCRβ locus. CD14 control PCR reactions are as in Figure 2.

(B) PCR analysis of Vβ-to-DJβ coding joints using various Vβ gene-specific primers on the indicated amounts of wild-type and core-RAG2 DNA purified from sorted DN3 pro-T cells.

(C) Diagram of reaction intermediates during TCRβ rearrangement with the blunt-ended linker (BW) shown ligated to cleaved 3′ Dβ, 5′ Dβ, and 3′ Vβ RSS ends. The linker primer BW-H and locus-specific primers (arrowheads) used in LMPCR are also shown.

(D) Linker-ligated DNA from wild-type or mutant DN3 and DN4 T cells was assayed by LMPCR for cleavage at the indicated RSS as depicted in (C).

(E) Comparison of 3′Dβ SBE in wild-type and mutant DN3 T cells as assayed by serial dilution followed by LMPCR as shown in (D).

each case, the frequency of dsDNA breaks was diminished in the mutant, but the appearance of breaks was appropriately limited to the DN3 stage. Finally, using an inverse PCR assay to detect signal joints, we ruled out the possibility that the decrease we observed in the frequency of SBEs in mutant cells was the result of unusually rapid generation of Vβ/Dβ signal joints (data not shown). Thus, the defect in TCRβ gene assembly in mutant thymocytes is remarkably similar to the defect in IgH gene assembly in mutant developing B cells.

γδ TCR Rearrangements in Core-RAG2 Mice

Along with attenuation of the DN3 to DN4 transition, we also observed a significant reduction of γδ T cells in core-RAG2 thymus (Figure S2A [http://www.immunity.com/cgi/content/full/17/5/639/DC1]). We found that TCR γ chain gene rearrangement was not affected but TCRδ rearrangement was affected by the core-RAG2 mutation (Figure S2C). Previous studies have shown that VDJδ rearrangement occurs during or before the DN4 stage of development (Hernandez-Munain et al., 1999). PCR analysis using Vδ and Jδ primers revealed a decrease in VDJδ rearrangement in core-RAG2 mutant DN3 and DN4 thymocytes (Figure S2B). In the TCR δ locus, Vδ-to-Dδ rearrangement often precedes VDδ-to-Jδ rearrangement, but the enhancer-dependent developmental regulation of the latter step makes it comparable to the V-to-DJ step in IgH and TCRβ rearrangement (Lauzurica and Krangel, 1994). Further analysis of rearrangement intermediates (Figure S2D) revealed that core-RAG2 thymocytes are defective in VDδ-to-Jδ rearrangement due to diminished cleavage at specific RSSs involved in this process.

Reduced Recombinase Activity in Core-RAG2-Expressing Cells

We considered several potential mechanisms to account for the selective defect in V-to-DJ rearrangement

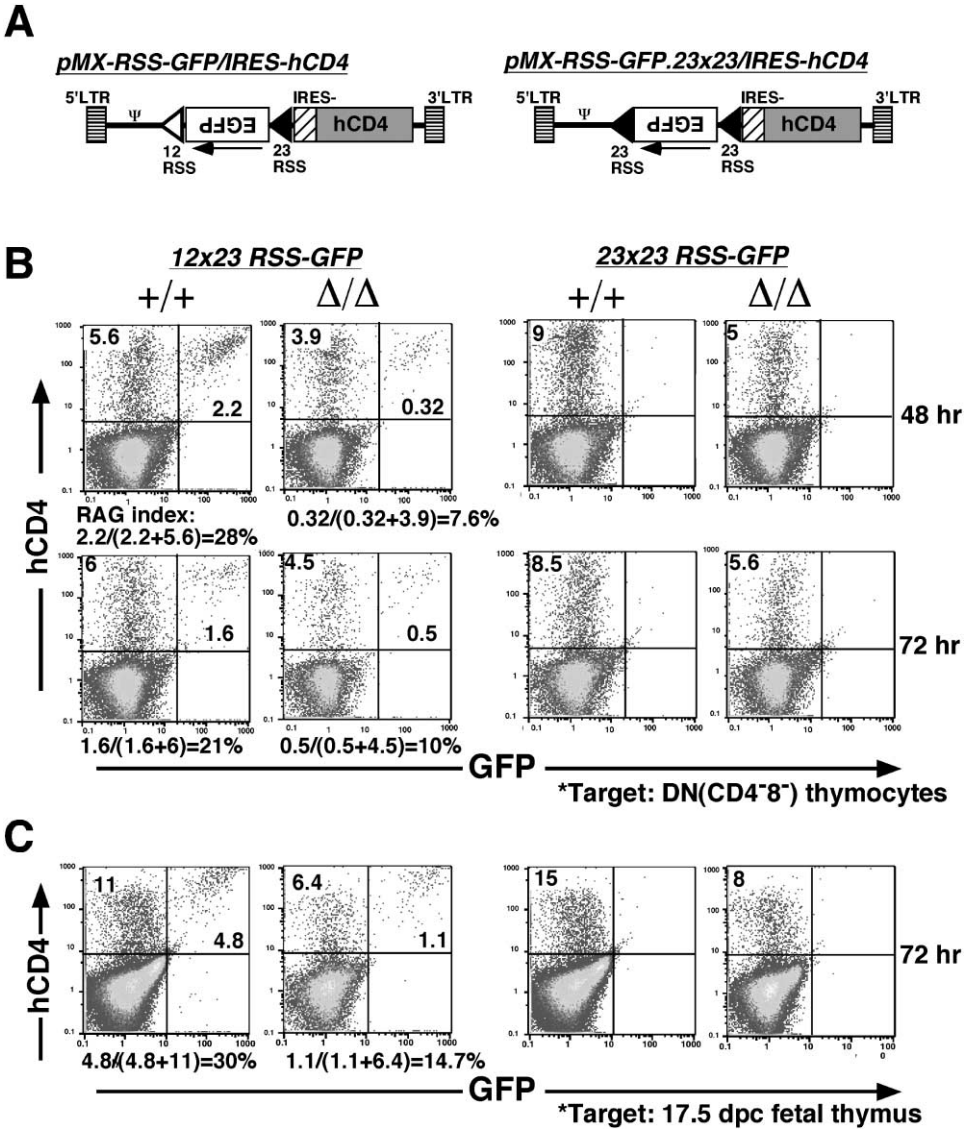

Figure 5. Diminished Core-RAG2 Recombinase Catalytic Activity Assayed Using a Retroviral Recombination Reporter

(A) Schematic representation of the retroviral vectors used as recombination reporters. The construct contains an anti-sense-oriented RSS-flanked EGFP reporter and an internal ribosomal entry site (IRES)-linked human CD4 (hCD4) cassette in the sense orientation. The 12- and 23-RSS are represented as open and closed triangles, respectively.

(B and C) MACS-purified DN thymocytes from adult wt (+/+) or core-RAG2 mutant (Δ/Δ) mice and total E17.5 embryonic thymocytes were infected with pseudotyped reporter viruses. At 48 or 72 hr postinfection, cells infected with either 12×23 RSS-GFP (left panel) or 23×23 RSS-GFP (right panel) reporter viruses were stained with PE-anti-hCD4, and simultaneous detection of GFP expression was performed by flow cytometry. Percentages shown are $hCD4^+$ and $hCD4^+GFP^+$ population out of live DN thymocytes. The RAG activity index was defined as the percentage of GFP^+ cells divided by the percentage of total $hCD4^+$ cells.

in core-RAG2 mice. First, it is possible that the catalytic activity of the core-RAG2-containing recombinase is significantly diminished and that the V-to-DJ recombination reaction requires optimal recombinase activity. Second, the non-core region of RAG2 may be involved in an aspect of RSS recognition, synapsis, or cleavage which is unique to V-to-DJ rearrangement. Finally, the non-core domain of RAG2 might be involved in the specific recruitment of the recombinase to V_H and Vβ gene segments. Perhaps more likely, the mutant phenotype might be due to a combination of these potential defects.

To examine whether differences in catalytic activity exist between the full-length and core-RAG2 containing recombinase complexes, we designed a reporter assay utilizing retroviral vectors to directly measure recombinase activity in developing lymphocytes (Figure 5A). The retroviral reporter integrates into the genome as proviral DNA, and the proviral LTR drives the production of a bicistronic transcript which allows for the simultaneous assessment of recombination (inversion of the RSS-GFP cassette and subsequent GFP expression) and infection efficiency (surface expression of hCD4 marker) on a single-cell basis.

The specificity and sensitivity of this assay was first confirmed by infecting thymocytes with either the 12×23

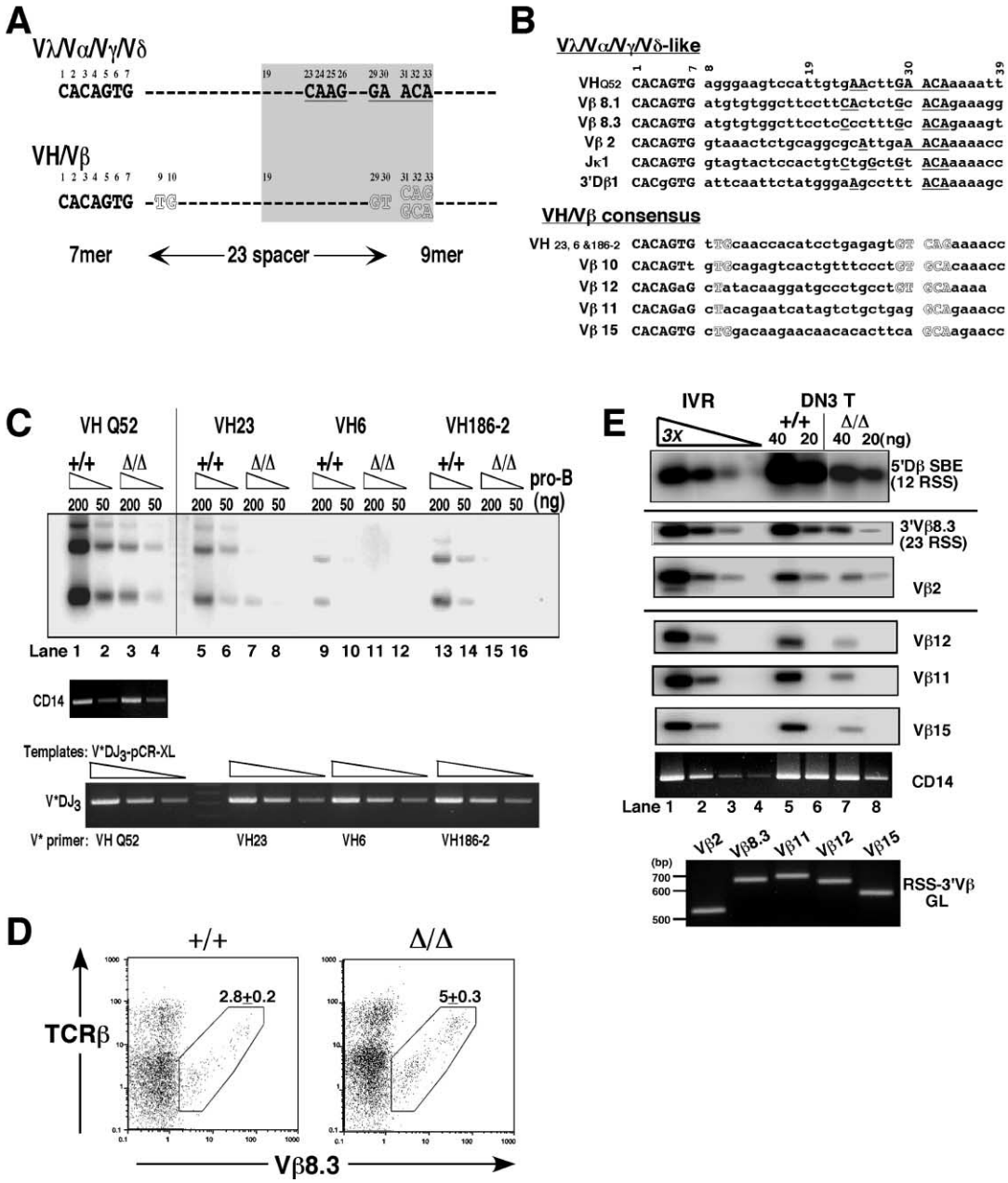

Figure 6. Most V_H and Vβ Gene Segments Show Relatively Inefficient Recombination Activity in Both Wild-Type and Core-RAG2 Mutant Lymphocyte Progenitors

(A) Comparison of consensus features of the 23-RSS from the Vλ/Vα/Vγ/Vδ genes with those of VH/Vβ origin. The shaded area represents nucleotides that show the most consistent differences between the two sets of 23-RSS (Cowell et al., 2002). Nucleotides characteristic of the Vλ/Vα/Vγ/Vδ consensus are underlined, and those of the VH/Vβ consensus are in outline.

(B) Sequence comparison of the two groups of 23-RSS derived from VH/Vβ genes used in this study. Within each group, the consensus nucleotides are highlighted (underlined capitals, Vλ/Vα/Vγ/Vδ-like; hollow capitals, VH/Vβ consensus). Heptamer nucleotides which differ from the canonical sequence are shown in lower case.

(C) PCR analysis of V-to-DJ_H coding joints utilizing four different V_H-gene-specific primers, VHQ52, VH23, VH6, and VH186-2, individually paired with a single downstream J_H primer. Twenty-three cycle PCR reactions were performed on 200 or 50 ng aliquots of genomic DNA purified from primary pro-B cell cultures. CD14, a 25-cycle control PCR visualized by EtBr gel; bottom, a 27-cycle control PCR on 250 ng 63-12 cell genomic DNA mixed with 1 ng, 50 pg, or 2.5 pg linearized pCR-XL plasmid containing a rearranged V^*DJ_{H3} insert amplified by the corresponding V_H-specific primer and downstream J_H primer. The same primer sets were also used to amplify the rearranged V^*DJ_{H3} fragments individually which were cloned into pCR-XL plasmid to serve as control templates.

(D) Thymocytes from 4-week-old wild-type (N = 6) or mutant (N = 4) mice were stained with FITC-anti-Vβ8.3 and PE-anti-TCRβ antibodies. Percentages are out of total live-gated thymocytes.

(E) DNA from either an in vitro RAG-mediated cleavage reaction (lanes 1–4) or from sorted wild-type (+/+) and core-RAG2 mutant (Δ/Δ) DN3 thymocytes (lanes 5–8) was analyzed by LMPCR for signal broken ends (SBE) at the indicated RSS. Three-fold serial dilutions of the linker-

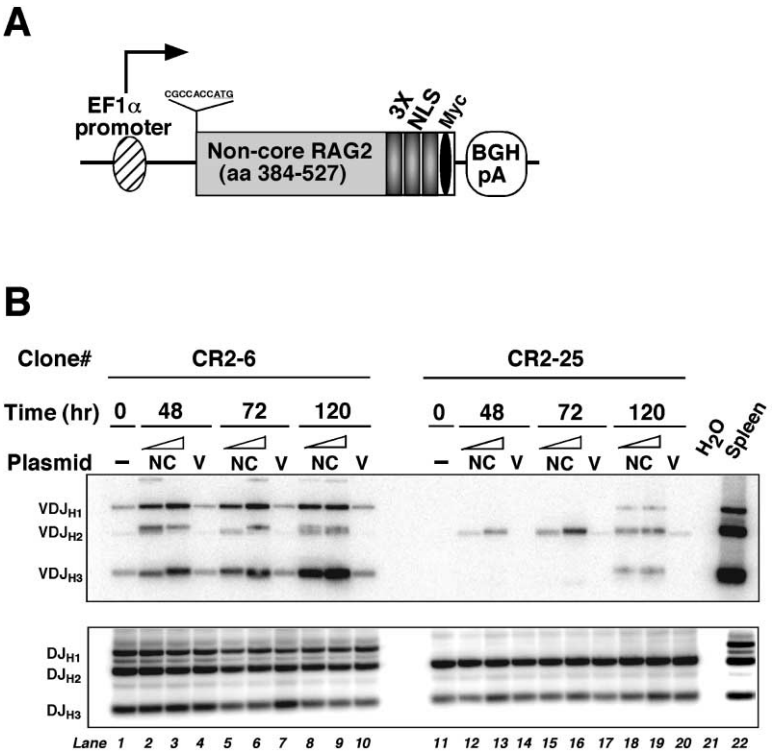

Figure 7. Overexpression of Non-Core RAG2 Is Associated with Increased Levels of V-to-DJ_H Rearrangement in v-*abl*-Transformed Core-RAG2 Pro-B Cells

(A) Diagram of the RAG2 non-core domain expression vector.

(B) Two AMuLV-transformed pro-B cell lines (CR2-6 and CR2-25) generated from core-RAG2 mutant bone marrow were transiently transfected with the non-core RAG2 expression vector (NC, 10 or 20 μg) or empty vector control (V, 10 μg). Genomic DNA was harvested at the indicated times and assayed for D-to-J and V-to-DJ rearrangements by PCR. Transfection efficiency was ~5% as determined by cotransfection of pEF/Nuc/GFP (Invitrogen).

(left panels) or the 23×23 (right panels) reporter viruses (Figures 5B and 5C). These two vectors supported similar levels of infection (total % of $hCD4^+$ cells), but the 23×23 vector failed to yield any detectable GFP signal, as expected. We used these reporter viruses to infect either adult DN (Figure 5B) or total fetal (Figure 5C) thymocytes from wild-type and core-RAG2 mice and calculated a RAG activity index as the percentage of GFP^+ cells divided by the percentage of total $hCD4^+$ cells. We found that core-RAG2 (Δ/Δ)-expressing cells display an approximately 2-fold reduction in recombinase activity relative to wild-type cells (Figure 5B, +/+ DN = 21% and Δ/Δ DN = 10%, respectively). The extent of reduction in the RAG activity index was even higher at an earlier time point (~3.7-fold at 48 hr), indicating that the kinetics of the core-RAG2-mediated reaction are slower. Similar results were obtained in assays using fetal thymocytes, although infection efficiencies were higher in this case (Figure 5C).

We also noticed that the infection efficiency of core-RAG2 thymocytes was consistently lower than that of wild-type targets. Given the fact that integration of the proviral reporter into the genome occurs only in dividing cells, we interpret this as being a reflection of the fact that fewer proliferating cells exist in the mutant sample. This is consistent with the defective β-selection observed in core-RAG2 thymus, which prevents the mutant DN3 cells from entering the proliferative phase (Figure 3B).

The Role of Recombination Signal Sequences in V-to-DJ Rearrangement

Our observation that the core-RAG2-containing recombinase has reduced activity but the mutation shows disproportional effects on different gene rearrangement events raised the possibility that subtle differences may exist between RSSs associated with different groups of gene segments, and these differences may contribute to the core-RAG2 mutant recombinase phenotype. We hypothesized that core-RAG2, a poor recombinase, might create a threshold effect among different RSS groups, and those affected by the core-RAG2 mutation during V-to-DJ rearrangement (3′VH RSS and 3′Vβ RSS, specifically) might display some unique feature in their nucleotide sequence when compared to other RSS groups which are recombined efficiently in the core-RAG2 mouse.

Based on this hypothesis, we simply divided 23-RSS from different V gene sets into two groups: VH/Vβ and Vλ/Vα/Vγ/Vδ. This grouping is determined by whether the rearrangement of a specific V gene set was affected by the core-RAG2 mutation. Then, using a novel statistical model of the RSS (Cowell et al., 2002), we analyzed 23-RSS within the VH/Vβ group (affected) and the Vλ/Vα/Vγ/Vδ group (unaffected). As summarized in Figure 6A, the most consistent differences between the two groups are: Vλ/Vα/Vγ/Vδ with CAAG at positions 23 through 26, and GAACA at positions 29 through 33; VH/

ligated in vitro-cleaved DNA (lanes 1–4) or two different amounts of DN3 cell DNA (lanes 5–8) were used to compare the relative abundance of different Vβ signal ends. Detection of 5′Dβ (12-RSS) signal ends from the same template DNA served as a positive control. RSS-3′Vβ, germline sequences 3′ of different Vβ genes were amplified by a 25-cycle PCR on 63-12 genomic DNA (100 ng) using RSS primers and the locus-specific primers used in primary LMPCR.

Vβ with TG at positions 9 and 10, and GTCAG or GTGCA at positions 29 through 33.

These analyses led us to predict that gene segments containing RSSs resembling the VH/Vβ consensus should recombine less frequently when compared to gene segments containing RSSs that more closely resemble the Vλ/Vα/Vγ/Vδ consensus. Figure 6B shows a collection of different VH/Vβ-associated RSSs that were categorized by their resemblance to either the VH/Vβ or Vλ/Vα/Vγ/Vδ consensus. The Jκ1 and 3′Dβ1 RSSs were found to be homologous to the Vλ/Vα/Vγ/Vδ-like consensus, also suggesting that this set of genes might display higher recombination efficiency since Igκ and TCR D-to-Jβ rearrangement were not affected by the core-RAG2 mutation.

To test our prediction, we compared the recombination efficiency of individual VH/Vβ gene-associated RSSs that either matched or diverged from the VH/Vβ consensus both in vivo and in vitro. Using a series of PCR assays designed to detect specific V-to-DJ gene rearrangements, we found that one specific V_HQ52 family gene (which has a Vλ/Vα/Vγ/Vδ-like RSS) rearranged more frequently in wild-type pro-B cells than those V_H gene segments (V_H23, V_H6, and V_H186-2; all from J558 family) flanked by the perfect VH/Vβ consensus RSS (Figure 6C, compare lanes 1 and 2 to 5 and 6, 9 and 10, and 13 and 14, respectively). Control experiments showed that each of these PCR assays was similarly efficient (Figure 6C, bottom) and displayed the intended V_H gene specificity based on PCR product sequencing (data not shown).

We found that each individual V_H gene rearrangement was reduced dramatically in core-RAG2 pro-B cells when compared to wild-type cells (lanes 1 and 2 versus 3 and 4 and lanes 5 and 6 versus 7 and 8, respectively), confirming the previously observed defect in V-to-DJ rearrangement. Most interestingly, preferential usage of the specific V_HQ52 gene segment was preserved in mutant cells, suggesting that the core-RAG2 complex could also distinguish between VH/Vβ consensus and nonconsensus RSSs.

We next extended our analysis to Vβ gene segment-associated RSS. First, we assayed the preference of the recombinase for individual Vβ RSS (Vβ 2, 8.1, 8.3, 11, 12, and 15) by reacting purified genomic DNA from a RAG-deficient pro-B cell line (germline configuration) with recombinant core-RAG1 and core-RAG2 in vitro. SBEs were assayed by Vβ-specific LMPCR assays (Figure 6E, lanes 1–4, and data not shown). We found that RSSs that matched the VH/Vβ consensus (Vβ11, Vβ12, and Vβ15) were cleaved less efficiently (about 3-fold) than those that more closely matched the Vλ/Vα/Vγ/Vδ consensus (Vβ 8.1, 8.3, and Vβ 2 RSS), while similar PCR efficiency was observed among the different assays (Figure 6E, bottom). DNA samples purified from DN3 thymocytes sorted from wild-type and core-RAG2 mice were also used to measure in vivo cleavage activity on specific Vβ RSS. The ex vivo results resemble those from in vitro cleavage assay in that the Vβ consensus RSSs are relatively poor substrates (Figure 6E, lanes 5–8). Also consistent with previous observations (Figure 4D), core-RAG2 DN3 cells are defective in cleaving the 5′Dβ 12-RSS and all the Vβ 23-RSS tested (Figure 6E, compare lanes 5 and 6 to 7 and 8).

These biochemical results led us to predict that Vβ gene segments whose RSSs more closely match the Vλ/Vα/Vγ/Vδ consensus would be expressed more frequently in core-RAG2 mice than in wild-type mice. FACS analysis revealed just such an increase in the frequency of Vβ8.3$^+$ T cells (∼1.8-fold, Figure 6D) and of Vβ2$^+$ cells (∼1.6-fold; data not shown) in core-RAG2 thymus. Thus, although the overall frequency of V-to-DJβ rearrangement is diminished in core-RAG2 mice, Vβ gene segments with Vλ/Vα/Vγ/Vδ consensus RSS fare the best, as predicted (Figure 6B). Taken together, these results lead us to conclude that, at least in part, the defect in V-to-DJ rearrangement observed in core-RAG2 mice reflects an effect of conserved features of most VH/Vβ RSS which make them uniquely sensitive to decreased recombinase activity.

The Non-Core Domain of RAG2 Can Complement the V-to-DJ$_H$ Rearrangement Defect Found in Core-RAG2 Pro-B Cells

In an attempt to further probe the role of the RAG2 non-core domain in V-to-DJ rearrangement, we tested whether expression of the non-core domain of RAG2 could complement the core-RAG2 mutant phenotype. We first generated progenitor B cell lines from core-RAG2 (Δ/Δ) mice by transforming mutant bone marrow with Abelson-murine leukemia virus (AMuLV). We screened cloned mutant AMuLV lines by PCR for the presence of preexisting VDJ_H coding joints. Two-thirds of the clones (13 out of 20 clones, data not shown) had at least some level of VDJ_H rearrangement, but all of them possessed DJ_H rearrangements on both IgH alleles (data not shown). We selected two clones that initially had DJ_H but not VDJ_H alleles for further study. We transiently transfected these core-RAG2 pro-B cell lines with either an empty expression vector or an expression vector encoding the non-core domain of RAG2 (Figure 7A). We observed a non-core RAG2 dosage- and time-dependent complementation of the mutant phenotype (Figure 7B, compare lanes 12, 13, 15, and 16 to 18 and 19, respectively). The ability of the non-core RAG2 to act in *trans* in cooperation with the core region of RAG2 has implications for its role in facilitating V(D)J recombination which might involve the interaction of this non-core RAG2 domain with RAG proteins and with other cellular targets.

Discussion

The potential functions of the highly conserved non-core region of RAG2 are of substantial interest (reviewed by Fugmann et al., 2000). We report here that endogenous IgH and TCRβ V-to-DJ rearrangement is greatly depressed in the absence of the RAG2 C terminus and that this selective defect affects proximal and distal V_H/Vβ gene segments equivalently. Inefficient IgH and TCRβ gene assembly results in a partial block in early B and T cell development at the precise stage when productively rearranged IgH and TCRβ gene products are essential for delivering developmental cues and promoting further differentiation.

Regulation of Recombinase Accessibility in Core-RAG2 Mice

The V(D)J recombination reaction is regulated in a tissue, lineage, and developmental stage-specific manner (Hesslein and Schatz, 2001; Sleckman et al., 1996). Although in some cases this regulation may occur at postcleavage steps (Hempel et al., 1998), it is primarily the DNA recognition/cleavage step of the reaction that is regulated by controlling the accessibility of RSSs to the common lymphoid recombinase (Stanhope-Baker et al., 1996). This occurs through, among other things, changes in chromatin structure, DNA methylation, or germline transcription that restrict or enhance RSS cleavage by the recombinase (Hesslein and Schatz, 2001; McMurry and Krangel, 2000; Sleckman et al., 1996).

By analyzing V(D)J recombination intermediates in DNA purified from sorted B and T cells at different developmental stages, we found that the control of recombinase accessibility among the various rearranging loci is not perturbed by the truncation of RAG2. We failed to observe precocious cleavage products derived from IgL chain gene segments in pro-B cells or the persistence of TCRβ locus or IgHC locus cleavage products in DN4 or pre-B cells, respectively (Figures 2E and 4D). Thus, the lineage and stage specificity, and allelic exclusion of V(D)J recombination are not affected by the core-RAG2 mutation. Rather, the locus- and stage-specific recombination phenotype reported here arises from defective recognition or cleavage of RSSs associated with the V-to-DJ step in antigen receptor gene assembly (Figures 2F and 4D).

Possible Mechanisms for the Selective Effects of Core-RAG2 Protein on V-to-DJ Rearrangement

A number of models could explain the dependence of efficient V-to-DJ rearrangement on the RAG2 C terminus. Full-length RAG2 might rely on this region to gain direct access to the site of rearrangement, perhaps by displacing previously bound factors. Alternatively, the insolubility of full-length RAG2 in vitro along with the clustering of acidic residues within the non-core region also suggests the potential engagement of this region of the protein with other structures in vivo (Levchenko et al., 1997; Steen et al., 1999). In the context of V-to-DJ rearrangement, the non-core region of RAG2 may play a significant role in the recruitment of other factors involved in targeting recombination, for example chromatin remodeling activities as suggested previously (Kirch et al., 1998). Alternatively, the non-core region might interact with lineage- or locus-specific transcription factors, helping recruit the recombinase complex to specific gene segments in a developmentally regulated fashion. It is also possible that the core-RAG2 mutation results in delayed cell cycle progression or enhanced cell death among early, cycling pre-B and pre-T cells due to the absence of its C-terminal degradation signal (Li et al., 1996).

We observed an approximately 2- to 3-fold reduction in catalytic activity of the core-RAG2-containing recombinase using a novel assay that directly measures recombinase activity in developing lymphocytes (Figure 5). This diminished activity leads us to suggest that the V-to-DJ phenotype might be due at least in part to quantitative alterations of core-RAG2 recombinase activity per se as compared to that of full-length RAG2. The differential susceptibility among rearranging loci to this reduced catalytic activity suggests that unique features of RSS associated with affected genes might also contribute to the phenotype. This hypothesis is consistent with mounting evidence for genetic patterning of the naive receptor repertoire including the biased use of certain gene segments within a given locus (Connor et al., 1995; Williams et al., 2001) and preferential synapse formation between certain pairs of RSSs (Bassing et al., 2000). In these cases, the control elements appear to be related to the specific nucleotide composition of the flanking RSS.

To test our hypothesis, we applied a novel statistical model that predicts the ideal RSS and quantifies the variation between any sequence and this ideal (Cowell et al., 2002). Of particular interest is the ability of this model to predict the recombination efficiency of RSS sequences that differ at the 23-spacer. This model predicts the preferential gene usage within a given locus shown in previous studies including the superiority of the RSS from V_H7183 family over those from V_HJ558 family (Williams et al., 2001) and in vivo RAG cleavage activity among different Vβ segments (Tillman et al., 2002, and this study). In addition, this model predicts that most V_H and Vβ 23-RSSs are relatively poor recombination substrates as compared to Vα, Vλ, and Jκ 23-RSSs. Thus, perhaps in addition to other factors, we propose that a synthetic interaction between an inefficient enzyme (core-RAG2) and poor substrates (V_H and Vβ RSS) may contribute to the core-RAG2 V-to-DJ rearrangement phenotype. In the case of the unaffected gene rearrangements (D-to-J and V-to-J), even diminished levels of enzyme activity appear sufficient to catalyze normal amounts of recombination.

Complementation of the Core-RAG2 Mutant Phenotype

To our surprise, we found that the non-core domain of RAG2 was able to complement the V-to-DJ rearrangement phenotype of the core-RAG2 mutant recombinase in a cell line-based assay system (Figure 7). This result suggests that the non-core domain of RAG2 is soluble and sufficiently stable within the cell to physically interact with the mutant recombinase and perhaps with other nuclear components as well. This non-core domain, however, is insoluble in vitro, thus precluding a biochemical investigation of its interaction with the recombinase (data not shown). We are currently examining wild-type developing B cells in which we have overexpressed the non-core domain of RAG2 by transgenesis for potential dominant-negative phenotypes which might reveal the nature of its interacting partners in the cell.

Potential Implications

Allelic exclusion, the observation that a functional gene product is produced by only one of the alleles of a rearranging locus in a given cell is most tightly enforced at the V-to-DJ step of IgH and TCRβ gene assembly. While there is clear evidence that accessibility of the heavy-chain locus is diminished in pre-B cells, the existence of an allele-specific or even reversible regulatory

mechanism controlling the accessibility of VH/Vβ RSSs during V-to-DJ step in pro-B cells has yet to be demonstrated (Hesslein and Schatz, 2001). Our results strengthen the possibility that V-to-DJ rearrangement is inherently inefficient in comparison to V-to-Jα or V-to-Jκ rearrangement due to unique features conserved among most V_H and Vβ RSSs. This inefficiency likely contributes to the allelic exclusion of IgH and TCRβ expression since it decreases the likelihood of near-simultaneous V-to-DJ rearrangement on both alleles. This model predicts that the rare B and T cells which show allelic inclusion would contain at least one VDJ-rearranged allele which utilizes a V_H or Vβ gene segment associated with an RSS that more closely resembles the Vα/Vλ/Jκ RSS consensus.

Experimental Procedures

Targeting Vector Construction, Generation of Core-RAG2 Knock-In ES Cells, and Mice

Detailed procedures are given in the supplemental data available at http://www.immunity.com/cgi/content/full/17/5/639/DC1.

Flow Cytometry

Single-cell suspensions depleted of RBC by buffered NH_4Cl solution or Lympholyte-M sedimentation (Cedarlane) were first incubated with FcR blocker (2.4G2) and then stained with FITC-, PE-, PE-TxR-, Cyc-, and biotin-conjugated (bi) antibodies and analyzed by an Epics XL-MCL (Beckman Coulter). The following antibodies were used (BD PharMingen and CALTAG): FITC-anti-$IgM^{a/b}$ (II/41), -CD4 (RM4-5), -CD3ε (145-2C11), -Vβ8.3; PE-anti-B220 (RA3-6B2), -CD24/HSA (M1/69), -CD25 (PC61), -CD8 (53-6.7), -human CD4 (RPA-T4), Cyc-anti-CD44 (IM7), bi-anti-CD43 (S7, prepared by authors), -CD4 (RM4-5), and -CD8 (53-6.7) were also used. SA-conjugated Cyc or QuantumRed (SIGMA) was used to reveal bi-antibodies. For most FACS plots, ≥100,000 events were collected; dead cells were excluded by propidium iodide (SIGMA) staining or by forward and side scatter gating. Data were analyzed with either CellQuest (Beckton-Dickinson) or FlowJo (Tree Star, Inc.) software. For sorting pro-/pre-B cells, BM IgM^+ cells were first depleted by rat-anti-mouse IgM microbeads on AutoMACS column (Miltenyi Biotec) according to the manufacturer's instruction. For DN3/DN4 pro-T cells, thymocytes were first enriched for DN cells by depleting SP and DP cells with bi-anti-CD4 and bi-anti-CD8 followed by SA-microbeads and AutoMACS separation. Cell sorting was performed on an Epics Elite (Beckman Coulter). The purity of sorted population was verified by postsort analysis (≥2,000 cells analyzed) to exceed 99%.

PCR and LMPCR Analysis

Sorted cells were enumerated by hemocytometer, embedded in agarose-plugs, or lysed directly for genomic DNA extraction (Schlissel, 1998). Previously described PCR analyses detecting coding joints (CJ) from various antigen receptor loci were used (Hempel et al., 1998; Schlissel and Baltimore, 1989; Schlissel et al., 1991, 2000).

LMPCR for detection of in vivo-generated broken signal ends (SBE) was described previously (Constantinescu and Schlissel, 1997; Han et al., 1997; Hempel et al., 1998; Schlissel et al., 1993; Stanhope-Baker et al., 1996; Tillman et al., 2002). Semiquantitative analysis of the relative levels of CJ or SBE was performed with dilutions of the template DNA into genomic DNA from the RAG2 null pro-B cell line, 63-12 (a gift from Dr. Fred Alt). A typical 25-cycle control reaction (identical conditions, without adding 63-12 genomic DNA) was also run, using the CD14-L and CD14-R primers (Hempel et al., 1998; Schlissel et al., 1993) to amplify the unrearranged *CD14* gene.

Retroviral Recombination Reporter Assay

The standard retroviral reporter construct, pMX-RSS-EGFP, was a gift from Dr. David Schatz. This construct contains the 12- and 23-RSS from pJH200 (Lieber et al., 1988), separated by EGFP (Clontech) with inverted orientation relative to 5′LTR. The control version of this reporter, pMX-RSS-EGFP.23×23, is identical except that it contains a 23×23 pair of RSSs derived from p23×23 (Eastman et al., 1996). An IRES-human *CD4* (IRES-hCD4) cassette from the pMSCV-IRES-hCD4 (a gift from Drs. Ken Murphy and Bill Sha) was placed downstream of the RSS-EGFP reporter to generate pMX-RSS-EGFP/IRES-hCD4 and pMX-RSS-EGFP.23x23/IRES-hCD4 retroviral vectors. Recombination reporter viruses were produced in a packaging cell line by transient transfection. Pseudotyped virus was harvested at 48 hr posttransfection and used directly for infecting both adult DN thymocytes and total fetal thymocytes (E17.5) from wt or mutant mice. Target cells were incubated with viral supernatant containing 4 μg/ml polybrene (SIGMA), 50 ng/ml r-mIL-7, and 50 ng/ml recombinant stem-cell factor (r-SCF) (R&D Systems) at 10^6 cells/ml in 24-well plate. Spin infection was performed at 1400×g, 30°C for 90 min. Flow cytometric analysis of thymocyte cultures was performed at 48 and 72 hr postinfection.

In Vitro RSS Cleavage Assays

The efficiency of RAG-mediated cleavage at different 3′Vβ RSS was measured by in vitro cleavage assay on purified 63-12 genomic DNA followed by LMPCR exactly as described (Stanhope-Baker et al., 1996), and individual Vβ-specific primers were used (Tillman et al., 2002).

Oligonucleotides

V_H gene-specific primers (derived from CDR2 region) for VDJ_H coding joints PCR are: V_HQ52 (V_H101), 5′GTGATATGGAGTGGTGGAAGCA CAGAC 3′; V_H186-2, 5′AATAGTGGTGGTACTAAGTACAATGAG 3′; V_H6, 5′GGTAGTAGTAGTACTAACTACAATGAG 3′; V_H23, 5′AGCAAT GGTGGTACTAACTACAATGAG 3′. Accession numbers for individual V_H genes are: J00502, J00530, J00535, and J00534. Primers used in germline control PCR reactions are from positions 1-20 of each Vβ-RSS (Figure 6B).

Generation and Transfection of v-*abl* Transformed B Cell Lines

Bone marrow cells were obtained from a 4-week-old core-RAG2 (Δ/Δ) mouse and transformed with AMuLV (produced by transient transfection of packaging cells with v-*abl* retroviral vector) under the guidance of Dr. Naomi Rosenberg. Non-core RAG2 cDNA (aa 384–527, with an engineered start codon) was subcloned into pEF/Nuc/Myc (Invitrogen) to generate pEF/NC/Nuc/Myc, which encodes the recombinant non-core RAG2 protein with exogenous nuclear localization sequences and Myc-tag at C terminus. Transient transfection of 5×10^6 AMuLV cells with pEF/NC/Nuc/Myc vector was performed by electroporation (280V, 950 μF).

Acknowledgments

We thank Drs. Phil Leder and Fred Alt for the TC-1 ES cells, Dr. Yangsong Gu for ES cell technique, Dr. Hua Gu for pLZNeo vector, Drs. David Schatz, Alfred Lee, Ken Murphy, Bill Sha, and Naomi Rosenberg for the retroviral constructs, Dr. Stephen Desiderio for RAG2 antibody, and Mr. Hector Nolla for help with flow cytometry. This manuscript was improved by the helpful criticisms of various members of the Schlissel lab, several anonymous reviewers, and Drs. Astar Winoto and David Raulet. This work was funded by a grant from the NIH to M.S.S. (AI40227) and an Arthritis Foundation Biomedical Science Grant (M.S.S.).

Received: May 7, 2002
Revised: September 25, 2002

References

Akamatsu, Y., and Oettinger, M.A. (1998). Distinct roles of RAG1 and RAG2 in binding the V(D)J recombination signal sequences. Mol. Cell. Biol. *18*, 4670–4678.

Bassing, C.H., Alt, F.W., Hughes, M.M., D'Auteuil, M., Wehrly, T.D., Woodman, B.B., Gartner, F., White, J.M., Davidson, L., and Sleckman, B.P. (2000). Recombination signal sequences restrict chromosomal V(D)J recombination beyond the 12/23 rule. Nature *405*, 583–586.

Connor, A.M., Fanning, L.J., Celler, J.W., Hicks, L.K., Ramsden, D.A., and Wu, G.E. (1995). Mouse VH7183 recombination signal se-

quences mediate recombination more frequently than those of VHJ558. J. Immunol. *155*, 5268–5272.

Constantinescu, A., and Schlissel, M.S. (1997). Changes in locus-specific V(D)J recombinase activity induced by immunoglobulin gene products during B cell development. J. Exp. Med. *185*, 609–620.

Corcoran, A.E., Riddell, A., Krooshoop, D., and Venkitaraman, A.R. (1998). Impaired immunoglobulin gene rearrangement in mice lacking the IL-7 receptor. Nature *391*, 904–907.

Cowell, L.G., Davilla, M., Kepler, T.B., and Kelsoe, G. (2002). Identification and utilization of arbitrary correlations in models of recombination signal sequences. Genome Biol., in press.

Eastman, Q.M., Leu, T.M., and Schatz, D.G. (1996). Initiation of V(D)J recombination in vitro obeying the 12/23 rule. Nature *380*, 85–88.

Eastman, Q.M., Villey, I.J., and Schatz, D.G. (1999). Detection of RAG protein-V(D)J recombination signal interactions near the site of DNA cleavage by UV cross-linking. Mol. Cell. Biol. *19*, 3788–3797.

Fugmann, S.D., and Schatz, D.G. (2001). Identification of basic residues in RAG2 critical for DNA binding by the RAG1–RAG2 complex. Mol. Cell *8*, 899–910.

Fugmann, S.D., Lee, A.I., Shockett, P.E., Villey, I.J., and Schatz, D.G. (2000). The RAG proteins and V(D)J recombination: complexes, ends, and transposition. Annu. Rev. Immunol. *18*, 495–527.

Han, S., Dillon, S.R., Zheng, B., Shimoda, M., Schlissel, M.S., and Kelsoe, G. (1997). V(D)J recombinase activity in a subset of germinal center B lymphocytes. Science *278*, 301–305.

Hardy, R.R., Carmack, C.E., Shinton, S.A., Kemp, J.D., and Hayakawa, K. (1991). Resolution and characterization of pro-B and pre-pro-B cell stages in normal mouse bone marrow. J. Exp. Med. *173*, 1213–1225.

Hempel, W.M., Stanhope-Baker, P., Mathieu, N., Huang, F., Schlissel, M.S., and Ferrier, P. (1998). Enhancer control of V(D)J recombination at the TCRbeta locus: differential effects on DNA cleavage and joining. Genes Dev. *12*, 2305–2317.

Hernandez-Munain, C., Sleckman, B.P., and Krangel, M.S. (1999). A developmental switch from TCRδ enhancer to TCRα enhancer function during thymocyte maturation. Immunity *10*, 723–733.

Hesslein, D.G., and Schatz, D.G. (2001). Factors and forces controlling V(D)J recombination. Adv. Immunol. *78*, 169–232.

Kirch, S.A., Sudarsanam, P., and Oettinger, M.A. (1996). Regions of RAG1 protein critical for V(D)J recombination. Eur. J. Immunol. *26*, 886–891.

Kirch, S.A., Rathbun, G.A., and Oettinger, M.A. (1998). Dual role of RAG2 in V(D)J recombination: catalysis and regulation of ordered Ig gene assembly. EMBO J. *17*, 4881–4886.

Landree, M.A., Wibbenmeyer, J.A., and Roth, D.B. (1999). Mutational analysis of RAG1 and RAG2 identifies three catalytic amino acids in RAG1 critical for both cleavage steps of V(D)J recombination. Genes Dev. *13*, 3059–3069.

Lauzurica, P., and Krangel, M.S. (1994). Enhancer-dependent and -independent steps in the rearrangement of a human T cell receptor delta transgene. J. Exp. Med. *179*, 43–55.

Levchenko, I., Yamauchi, M., and Baker, T.A. (1997). ClpX and MuB interact with overlapping regions of Mu transposase: implications for control of the transposition pathway. Genes Dev. *11*, 1561–1572.

Li, Z., Dordai, D.I., Lee, J., and Desiderio, S. (1996). A conserved degradation signal regulates RAG-2 accumulation during cell division and links V(D)J recombination to the cell cycle. Immunity *5*, 575–589.

Lieber, M.R., Hesse, J.E., Lewis, S., Bosma, G.C., Rosenberg, N., Mizuuchi, K., Bosma, M.J., and Gellert, M. (1988). The defect in murine severe combined immune deficiency: joining of signal sequences but not coding segments in V(D)J recombination. Cell *55*, 7–16.

Lin, W.C., and Desiderio, S. (1993). Regulation of V(D)J recombination activator protein RAG-2 by phosphorylation. Science *260*, 953–959.

McMahan, C.J., Difilippantonio, M.J., Rao, N., Spanopoulou, E., and Schatz, D.G. (1997). A basic motif in the N-terminal region of RAG1 enhances V(D)J recombination activity. Mol. Cell. Biol. *17*, 4544–4552.

McMurry, M.T., and Krangel, M.S. (2000). A role for histone acetylation in the developmental regulation of VDJ recombination. Science *287*, 495–498.

Mo, X., Bailin, T., and Sadofsky, M.J. (1999). RAG1 and RAG2 cooperate in specific binding to the recombination signal sequence in vitro. J. Biol. Chem. *274*, 7025–7031.

Naramura, M., Hu, R.J., and Gu, H. (1998). Mice with a fluorescent marker for interleukin 2 gene activation. Immunity *9*, 209–216.

Qiu, J.X., Kale, S.B., Yarnell Schultz, H., and Roth, D.B. (2001). Separation-of-function mutants reveal critical roles for RAG2 in both the cleavage and joining steps of V(D)J recombination. Mol. Cell *7*, 77–87.

Roman, C.A., Cherry, S.R., and Baltimore, D. (1997). Complementation of V(D)J recombination deficiency in RAG-1(−/−) B cells reveals a requirement for novel elements in the N-terminus of RAG-1. Immunity *7*, 13–24.

Schlissel, M.S. (1998). Structure of nonhairpin coding-end DNA breaks in cells undergoing V(D)J recombination. Mol. Cell. Biol. *18*, 2029–2037.

Schlissel, M.S., and Baltimore, D. (1989). Activation of immunoglobulin κ gene rearrangement correlates with induction of germline κ gene transcription. Cell *58*, 1001–1007.

Schlissel, M.S., Corcoran, L.M., and Baltimore, D. (1991). Virus-transformed pre-B cells show ordered activation but not inactivation of immunoglobulin gene rearrangement and transcription. J. Exp. Med. *173*, 711–720.

Schlissel, M., Constantinescu, A., Morrow, T., Baxter, M., and Peng, A. (1993). Double-strand signal sequence breaks in V(D)J recombination are blunt, 5′-phosphorylated, RAG-dependent, and cell cycle regulated. Genes Dev. *7*, 2520–2532.

Schlissel, M.S., Durum, S.D., and Muegge, K. (2000). The interleukin 7 receptor is required for T cell receptor gamma locus accessibility to the V(D)J recombinase. J. Exp. Med. *191*, 1045–1050.

Sekiguchi, J.A., Whitlow, S., and Alt, F.W. (2001). Increased accumulation of hybrid V(D)J joins in cells expressing truncated versus full-length RAGs. Mol. Cell *8*, 1383–1390.

Sleckman, B.P., Gorman, J.R., and Alt, F.W. (1996). Accessibility control of antigen-receptor variable-region gene assembly: role of cis-acting elements. Annu. Rev. Immunol. *14*, 459–481.

Stanhope-Baker, P., Hudson, K.M., Shaffer, A.L., Constantinescu, A., and Schlissel, M.S. (1996). Cell type-specific chromatin structure determines the targeting of V(D)J recombinase activity in vitro. Cell *85*, 887–897.

Steen, S.B., Han, J.O., Mundy, C., Oettinger, M.A., and Roth, D.B. (1999). Roles of the "dispensable" portions of RAG-1 and RAG-2 in V(D)J recombination. Mol. Cell. Biol. *19*, 3010–3017.

Swanson, P.C., and Desiderio, S. (1998). V(D)J recombination signal recognition: distinct, overlapping DNA-protein contacts in complexes containing RAG1 with and without RAG2. Immunity *9*, 115–125.

Swanson, P.C., and Desiderio, S. (1999). RAG-2 promotes heptamer occupancy by RAG-1 in the assembly of a V(D)J initiation complex. Mol. Cell. Biol. *19*, 3674–3683.

Tillman, R.E., Wooley, A.L., Hughes, M.M., Wehrly, T.D., Swat, W., and Sleckman, B.P. (2002). Restrictions limiting the generation of DNA double strand breaks during chromosomal V(D)J recombination. J. Exp. Med. *195*, 309–316.

von Boehmer, H., Aifantis, I., Feinberg, J., Lechner, O., Saint-Ruf, C., Walter, U., Buer, J., and Azogui, O. (1999). Pleiotropic changes controlled by the pre-T-cell receptor. Curr. Opin. Immunol. *11*, 135–142.

Williams, G.S., Martinez, A., Montalbano, A., Tang, A., Mauhar, A., Ogwaro, K.M., Merz, D., Chevillard, C., Riblet, R., and Feeney, A.J. (2001). Unequal VH gene rearrangement frequency within the large VH7183 gene family is not due to recombination signal sequence variation, and mapping of the genes shows a bias of rearrangement based on chromosomal location. J. Immunol. *167*, 257–263.